

Rhodopsin-Transducin Interface: Studies with Conformationally Constrained Peptides

Rieko Arimoto,* Oleg G. Kisselev,[†] Gergely M. Makara,* and Garland R. Marshall*

*Department of Biochemistry and Molecular Biophysics, Washington University, St. Louis, Missouri 63110, and

[†]Department of Ophthalmology, St. Louis University, St. Louis, Missouri 63104 USA

ABSTRACT To probe the interaction between transducin (G_t) and photoactivated rhodopsin (R^*), 14 analog peptides were designed and synthesized restricting the backbone of the R^* -bound structure of the C-terminal 11 residues of $G_t\alpha$ derived by transferred nuclear Overhauser effect (TrNOE) NMR. Most of the analogs were able to bind R^* , supporting the TrNOE structure. Improved affinities of constrained peptides indicated that preorganization of the bound conformation is beneficial. Cys347 was found to be a recognition site; particularly, the free sulfhydryl of the side chain seems to be critical for R^* binding. Leu349 was another invariable residue. Both Ile and *tert*-leucine (Tle) mutations for Leu349 significantly reduced the activity, indicating that the Leu side chain is in intimate contact with R^* . The structure of R^* was computer generated by moving helix 6 from its position in the crystal structure of ground-state rhodopsin (R) based on various experimental data. Seven feasible complexes were found when docking the TrNOE structure with R^* and none with R. The analog peptides were modeled into the complexes, and their binding affinities were calculated. The predicted affinities were compared with the measured affinities to evaluate the modeled structures. Three models of the $R^*/G_t\alpha$ complex showed strong correlation to the experimental data.

INTRODUCTION

G-protein-coupled receptors (GPCRs) are integral membrane proteins that transduce an extracellular event to an intracellular signal and are vitally important to many physiological functions, such as vision, olfaction, taste, and endocrine signaling. The primary intracellular interaction of a GPCR occurs with a signal-transducing, heterotrimeric G-protein, consisting of α , β , and γ subunits. The binding of an activated GPCR to the $G\alpha\beta\gamma$ catalyzes exchange of GTP for GDP bound to $G\alpha$. The $G\alpha\beta\gamma$ then leaves the GPCR as $G\alpha$ -GTP and $G\beta\gamma$ complex, both of which can trigger the proper intracellular events. Although the overall pathway is well established, the G-protein activation mechanism at atomic resolution remains unclear. A number of human diseases are characterized by mutations in GPCRs, and a large fraction of the therapeutic compounds in use are thought to interact with GPCRs. Understanding the interaction between a GPCR and its G-protein in detail potentially leads to a rational design of drugs to control the activities of GPCRs. The lack of structural information has hindered us from an atomic view of the interactions in the complex. Crystal structures of various G-proteins (Coleman and Sprang, 1998; Lambright et al., 1996; Tesmer et al., 1997; Wall et al., 1995) and dark-adapted rhodopsin, the GPCR in vision (R), have been solved (Palczewski et al., 2000). Direct determination of the structure of an activated GPCR or its complex, the signal-transducing state, has been im-

peded by lack of availability and/or stability of activated GPCRs, including rhodopsin.

Molecular modeling is an alternative way to estimate protein structure. Its ability to predict tertiary structures has improved due to the better algorithms, scoring functions based on rapidly expanding crystal-structure data, and increasing computer power (Moult et al., 1999). Prediction of small protein loops in homology modeling has seen significant progress (Galaktionov et al., 2001). Several molecular-docking programs (Gabb et al., 1997; Goodsell and Olson, 1990; Meng et al., 1992; Vakser, 1996) have been shown to find correct binding sites from separate structures of receptors and their ligands. Based on the vast biochemical studies that have been carried out on the interactions between many different GPCRs and G-proteins, we believe that molecular modeling has a potential to integrate the diverse experimental observations and construct feasible models of the interface between G-proteins and their receptors.

Rhodopsin-transducin (G_t) is the typical, and the most extensively studied, G-protein-linked signal transduction system. Light triggers the signaling cascade with photoisomerization of 11-*cis* retinal, a small-molecule chromophore covalently attached to Lys296 of rhodopsin, into the all-*trans* form. Rhodopsin undergoes conformational changes into the activated state (R^*) that can bind and activate G_t . The activation of rhodopsin and the binding of G_t can be monitored by UV/visible spectroscopy. The absorbance peak of rhodopsin shifts from 500 nm (R) to an equilibrium between 490 nm (Meta I) and 380 nm (Meta II) upon activation, and the binding of G_t stabilizes Meta II and shifts the equilibrium toward 380 nm. To understand the G_t -activation mechanism, the structural change during $R \rightarrow R^*$ needs to be determined first and then the binding of G_t to rhodopsin can be modeled as G_t binds only to R^* .

Received for publication 5 June 2001 and in final form 4 September 2001.

G. M. Makara's current address: NeoGenesis, Inc., Cambridge, MA 02139.

Address reprint requests to Dr. Garland R. Marshall, Department of Biochemistry and Molecular Biophysics, Washington University, St. Louis, MO 63110. Tel.: 314-362-1567; Fax: 314-747-3330; E-mail: garland@pcg.wustl.edu.

© 2001 by the Biophysical Society

0006-3495/01/12/3285/09 \$2.00

As to the conformational change, Farrens et al. (1996) proposed rigid motion of helix 6 based on electron paramagnetic resonance (EPR) experiments measuring distances between residues on the cytoplasmic ends of helix 3 and helix 6 during light activation. Tracing the movement of retinal analogs in rhodopsin by photoaffinity as rhodopsin changed its absorbance peak from 500 nm to 380 nm, Borhan et al. (2000) found that the ionone ring of the retinal cross-linked to Trp265 on helix 6 in R and to Ala169 on helix 4 in R*. They suggested that helix 4 had to rotate slightly to orient Ala169 toward the ionone ring, and helix 3 had to move because the all-*trans* retinal would have negative steric interactions otherwise. As the crystal structure of R (Palczewski et al., 2000) subsequently revealed that helix 3 was highly tilted, this might not be the case.

It has been implicated that all of the cytoplasmic domains, except for the first loop connecting helices 1 and 2, are involved in the interaction with G_t (Hamm et al., 1988; Hargrave et al., 1993). Tyr136-Val139 in loop 2, Glu247-Thr251 in loop 3 (Acharya et al., 1997), Asn310-Gln312 in loop 4 (Marin et al., 2000; Ernst et al., 2000) (the crystal structure revealed an eighth helix running parallel to the disk membrane), and the C-terminal tail (Takemoto et al., 1986; Phillips and Cerione, 1994) have been pointed out as potential interaction sites by mutational analysis and peptide competition assay. On transducin, both G_tα and G_tβγ complex appear to contact with R*. The N-terminal 23 residues, internal sequence, and the C-terminal 11 residues in G_tα (Hamm et al., 1988) and the C-terminal 12 residues of G_tγ (Kisselev et al., 1995) are the known sites of interaction. It was demonstrated that synthetic peptides corresponding to the C-termini of G_tα (IKENLKDCGLF) and G_tγ (DKNPFKELKGGC-farnesylated) bind to R* and stabilize Meta II, mimicking the effect of G_t.

The R*-bound structure of G_tα(340–350) has been determined by transferred nuclear Overhauser effect (TrNOE) NMR spectroscopy (Dratz et al., 1993; Kisselev et al., 1998). In the case of the studies by Dratz et al. (1993), the peptide used was an analog (IRENLKDCGLF) with higher affinity for R*. This higher affinity appears to have an exchange rate far from the optimum for the TrNOE experiment resulting in suboptimal spectra leading to a misassignment of resonances and a wrong conclusion concerning the R*-bound structure that was ultimately acknowledged (Dratz et al., 1997). The native sequence used by us (Kisselev et al., 1998) has the exchange characteristics appropriate for obtaining optimal TrNOE spectra, and the resulting structure is unambiguous. When a higher-affinity analog (VLEDLKSCGLF) was subjected to the same experimental conditions, little useful information was obtained. In summary of the results obtained by Kisselev et al. (1998), G_tα(340–350) binds to photoactivated rhodopsin to form a continuous helix terminated by a reverse glycine C-cap turn (Schellman, 1980) with a distinctive hydrophobic cluster of the side chains of two leucines, a lysine, and

a phenylalanine. Based on the conservation of these residues in most subclasses of G-proteins, this motif may be of significance in GPCR/G-protein interactions, at least for the rhodopsin family of GPCRs. In fact, the corresponding C-terminal region in the crystal structure of G_iα, rhodopsin-family G-protein (Tesmer et al., 1997), showed identical conformation to the TrNOE-derived structure (Kisselev et al., 1998). Nevertheless, Hamm and her colleagues (Aris et al., 2001) continue to question the results from the Kisselev et al. (1998), citing inherent problems in interpretation of TrNOE experiments. To confirm the relevance of the TrNOE-derived structure of Kisselev et al. (1998), we decided to stabilize the deduced conformation by chemical modification to determine if Meta II stabilization was retained in such analogs.

Structure-activity studies have been carried out on the G_tα(340–350)-rhodopsin system by a combinatorial approach using phage display and random single amino-acid substitution of the IKENLKDCGLF sequence (Martin et al., 1996; Aris et al., 2001). The results revealed that substitution of Lys341 with a Leu markedly improved binding. This is in agreement with the hypothesis that the protonated side chain of Lys341 plays a crucial role in the hydrophobic cluster, providing an energy cost of deprotonation upon R* binding to maintain the affinity of transducin within the optimal range for its biological role. Further evidence that Lys341 binds in the unprotonated state comes from studies on a series of Phe350 mutation analogs with *para*-Phe substituents (Sha et al., 2001). The availability of the experimental data (Kisselev et al., 1998) on the three-dimensional structure of the G_tα(340–350) enabled us to investigate the structure-activity relationships in greater detail. Thus, we have designed 14 peptides based on the TrNOE structure (Kisselev et al., 1998). The analogs were designed to stabilize the peptide-backbone structure and vary in their surface structure, so that the binding site of R* could be probed. Starting with the crystal structure of R, the structural change upon light activation was simulated based on current experimental data to generate a model of the R* structure. Molecular docking technique was then able to build hypothetical complexes of G_tα(340–350)/R* that are feasible sterically and electrostatically. When affinity predictions using VALIDATE (Head et al., 1996) for the hypothetical complexes were compared with the measured affinities, the plausibility of the models could be evaluated. From these studies, atomic-resolution models of the interface between R* and transducin are proposed.

EXPERIMENTAL PROCEDURES

Design of peptide analogs

A list of the designed analogs is shown in Table 1. The disulfide bridges of analogs 1c and 2c were used to stabilize the glycine C-cap turn moiety (Schellman, 1980). The penicillamine (Pen) in analog 1 is for retaining the hydrophobicity of the Leu349 side chain due to the two methyl groups and

TABLE 1 Structures and binding affinities of the synthetic peptides

	Analog structure	EC ₅₀	
		-DTT (c)	+DTT
1c, 1	IKENLKDcyclo(CGPen)F	5 mM	10 mM
2c, 2	IKENLKDcyclo(CGC)F	≫10 mM	≫10 mM
3	IKENLKDP(D-NMeAla)LF		≫10 mM
4	IKENLKD(3Mpt)GLF		≫10 mM
5	IKENLKDC(D-Ala)LF		400 μM
6c, 6	IKEcyclo(CLKDC)GLF	≫10 mM	200 μM
7	AibKAibAibLKDCGLF		700 μM
8	IKcyclo(ENLK)DCGLF		70 μM
9	MLENLKDCGLF		25 μM
10	MLENLKDCGLF-CH ₂ OH		75 μM
11	VLEDLKSCGLF		5 μM
12	IKENLKDSGLF		≫10 mM
13	IKENLKDCGIF		6 mM
14	IKENLKDCGTleF		9 mM
15	Gtα(340–350); IKENLKDCGLF		500 μM

provides a site for disulfide constraint. The Pro-D-NMeAla dipeptide sequence of analog 3 has previously been predicted (Chalmers and Marshall, 1995; Takeuchi and Marshall, 1998) to have a high reverse turn propensity in aqueous media by Monte Carlo/stochastic dynamics calculations (Guarnieri and Still, 1994). Because a peptide with Gly348 replaced with D-Ala (analog 5) has been shown to retain full activity (Dratz et al., 1993), the use of a D-Ala derivative seemed justified. 3-Mercaptoproline (3Mpt) (Kolodziej et al., 1995) in analog 4 combines the high turn propensity of proline with the required side chain functionality of cysteine. Analog 6c contains a helix-stabilizing disulfide bond in the helical region of G_tα(340–350). 1-Aminoisobutyric acid (Aib, α-methylalanine) has long been known (Marshall and Bosshard, 1972; Hodgkin et al., 1990) to favor helical secondary structures as a result of deletion of allowed conformational regions in the Ramachandran plot due to the bulk imposed by the α-methyl groups. Thus, three of the residues in the helical region were substituted by Aib in analog 7. Amide bond formation between the side chains of Lys and Glu (analog 8) or Asp has been reported to provide up to 30-fold gain in binding energy (Miranda et al., 1997) due to a decrease in the conformational entropy of a helical peptide segment. Highly populated helices with reduced temperature dependence have also been observed on circular dichroism spectra for similar sequences. As removal of the positive charge carried by the amino side chain of Lys341 from the hydrophobic cluster has been reported to increase the affinity (Martin et al., 1996; Aris et al., 2001) (analogs 9 and 11), elimination of the closely positioned negatively charged carboxyl C-terminus (analog 10) may give rise to a similar effect by reduction of the desolvation free energy. Potential roles of the side chains of Cys347 and Leu349 were examined by point mutations in peptides 12–14.

Initial structures of the analogs were built by modifying the R*-bound structure (Kisselev et al., 1998). The GB/SA continuum model (Still et al., 1990) was used with extended electrostatics and force field charges to simulate aqueous solvation. The ring systems in the analogs possessing constrained cyclic motifs were subjected to Monte Carlo/molecular dynamics search (Guarnieri and Still, 1994) to explore all energetically reasonable conformations. Amide bonds were kept in the *trans* conformation while all other torsional angles between heavy atoms were varied by 60°–180° in each Monte Carlo move. The structures within 30 kcal/mol from the global minimum were compared with the corresponding region of the TrNOE structure. This procedure was able to isolate unfavorable ring designs. All calculations were carried out using Macromodel 5.5 (Mohamadi et al., 1990) with the Amber94 force field (Cornell et al., 1995) on Silicon Graphics Indigo R4000 and R10000 workstations.

Peptide synthesis

Analog peptides were synthesized with standard solid-phase methodology by manual or automatic Fmoc strategy. Coupling was facilitated by *O*-benzotriazol-1-yl-*N,N,N',N'*-tertamethyluronium tetrafluoroborate/1-hydroxybenzotriazole/diisopropylethylamine (TBTU/HOBt/DIEA) reagents, and 25% piperidine in *N,N'*-dimethylformamide was used for deprotection. The crude peptides were released from the Wang-resin (2-Cl-trityl-resin for analog 10) by the following cocktail: 90% trifluoroacetic acid (TFA), 5% water, 2.5% 1,2-ethanedithiol (EDT), 2.5% anisole. For the methionine-containing peptides (analogs 9 and 10), anisole was replaced by thioanisole. Analog 4 was synthesized on the Merrifield-resin and isolated as a mixture of two diastereomers. Boc-protected *trans*-3-(*p*-methylbenzylmercapto)proline (Kolodziej et al., 1995) was coupled manually (two-fold excess) with TBTU/HOBt/DIEA reagents overnight. The Boc group was removed by 50% TFA/dichloromethane, and the synthesis was completed on the ACT396 synthesizer (Advanced ChemTech, Louisville KY). Analog 8 was synthesized on the Merrifield-resin. The peptide was treated with TFA after coupling Glu342, to remove the protecting groups of the two side chains (Glu342 and Lys345) whereas all other protecting groups including the linker to the resin remained intact. The two side chains were cyclized with TBTU/HOBt/DIEA, and then the synthesis of the protected cyclic peptide was completed on the resin support. Final cleavage of analogs 4 and 8 was done with HF (2.5% anisole, 2.5% EDT) for 1 h at 0°C. The disulfide bridges were formed by stirring the crude peptides in 20% dimethylsulfoxide/water solution for 12 h, and then the mixtures were lyophilized. All crude peptides were purified to 95%+ purity by preparative reverse-phase high-performance liquid chromatography (HPLC) using C4 or C18 column (solvent A: 0.1% TFA in H₂O; solvent B: 100% acetonitrile; gradient: 20–55% in 20 min). Methionine-containing peptides were chilled to –78°C immediately after fraction collection because of their observed susceptibility to oxidation. The pure peptides were eluted at 37–47% B and analyzed by electrospray mass spectrometry. Criteria to establish purity were 95%+ peak area in analytical HPLC and no peak in the mass spectrum besides the target molecular weight, double-, triple-charged, and sodium- or potassium-complexed peaks.

UV/visible spectroscopy

The binding affinities of the analog peptides were measured using a Meta II stabilization assay (Kisselev et al., 1995) by UV/visible spectroscopy. The assay samples contained 100 μg/ml (~2.5 μM) of rhodopsin in rod outer-segment membranes, prepared as described (Papermaster and Dreyer, 1974; Yamazaki et al., 1982), and analog peptides in buffer A (pH 8.0, 20 mM Tris/HCl, 130 mM NaCl, 1 mM MgCl₂, 1 μM EDTA, 2 mM dithiothreitol (DTT)). The assays were done with and without DTT for analogs containing disulfide constraints. With DTT, the peptide solutions (in buffer A) were incubated for 3 h under N₂ at room temperature before the experiment to break the disulfide bonds. The samples were kept on ice at 0°C and prepared under dim red light or in the dark to avoid premature bleaching of rhodopsin. The absorption spectrum of dark-adapted rhodopsin was taken, and rhodopsin was activated by 490 ± 5 nm light for 20 s, followed by a scan acquiring the second spectrum, using a Cary50 spectrophotometer (Varian, Palo Alto, CA). The cuvette compartment was maintained at 4°C. The measurements were repeated with increasing concentration of analog peptides from 1 μM up to 5 mM. The Meta II stabilization was calculated as ΔA_{380 nm} – ΔA_{417 nm}, where ΔA is the absorbance change before and after light activation.

Modeling photoactivated rhodopsin

As some of the residues in loop 3 of dark-adapted rhodopsin are disordered in the crystal structure (Palczewski et al., 2000), they were

TABLE 2 Distances between Val139 and Lys248 to Arg252

Val139 to	EPR <i>R</i>	X-ray <i>R</i>	EPR <i>R</i> *	Estimated <i>R</i> *	Model <i>R</i> *
Lys248	12–14	8.5	23–25	15.6	14.4
Glu249	15–20	11.5	15–20	11.5	11.5
Val250	15–20	10.35	12–14	8.5	10.1
Thr251	12–14	8.33	23–25	15.6	13.8
Arg252	15–20	11.5	23–25	15.6	14.8

*Distances are in angstroms.

restored with standard loop reconstruction approaches (Galaktionov et al., 2001) to provide a complete atomic resolution model of R. A model of the R* structure was obtained by moving helix 6 (Lys245-Phe276) in the crystal structure (Palczewski et al., 2000) of R. A rigid-body motion of helix 6 was predicted by EPR experiments (Farrens et al., 1996) measuring the distances between residues on the cytoplasmic ends of the helices 3 and 6, before and after light activation of rhodopsin. In columns 1 and 2 of Table 2, EPR-measured values (Farrens et al., 1996) for R and the corresponding distances in the x-ray crystal structure (Palczewski et al., 2000) are listed. Although the relative distances are similar, the absolute values of the distances are quite different. This is likely because distances were measured between the α -carbons (C α s) in the crystal structure (Palczewski et al., 2000), whereas EPR used nitroxide spin labels located five rotatable bonds away from the C α s (Farrens et al., 1996). This problem is exemplified in the distance between two spin labels on Cys140 and Cys316 estimated at 37 Å (Delmelle and Virmaux, 1977) when the measured distance between the two C α s in the crystal structure is only 29 Å. The experimental data with R* (column 3) was scaled to improve the correspondence between EPR data and crystal structure measurements, to obtain the target distances (column 4) using the following formula:

$$\text{Estimated } R^* = \overline{\text{EPR } R^*} \times (\text{x-ray } R / \overline{\text{EPR } R}).$$

Helix 6 with a part of the cytoplasmic loop 3, consisting of Ser240-Phe276, was moved to a location where the root mean square error from the target distances and the deviation from the crystal structure were both minimized. The amide bond of Phe276 to Thr277 was then restored, and the residues Gln236-Glu239 (missing in the crystal structure) were modeled (Galaktionov et al., 2001) in between Ser240 of R* and Ala235 of R. The crystal structure of dark-adapted rhodopsin was, thus, minimally modified to include the experimentally observed changes by EPR (Farrens et al., 1996) in the relative positions of helices 3 and 6. The structures of cytoplasmic loop 3 and extracellular loop3 were energy minimized with the Kollman force field (Hall and Pavitt, 1984), allowing residues Gln236-Thr243 and 275–281 to accommodate the impact of helix 6 movement. The molecular modeling was performed using Sybyl 6.5 (Tripos, St. Louis, MO) on a Silicon Graphics Indigo R10000 workstation.

Modeling the R*-G α interface

The TrNOE structure of G α (340–350) was docked as a rigid body into the cytoplasmic face of modeled R*, consisting of four loops, Tyr60-Leu76, Val130-Thr160, Gln225-Arg252, and Ile305-Cys322, using FTDOCK program (Gabb et al., 1997). The C-terminal segment after the palmitoylation sites at Cys322 and Cys323 was omitted because 1) its structure is not well defined as the crystal structure is missing residues Leu328-Ala333 and 2) the segment of Ser334-COOH is distant from the hypothetical binding site described below. G α (340–350) was scanned over the space around the R*-loops, exploring the six degrees of freedom at a resolution of 1.2 Å and 20°. Structures of the complexes were scored by the surface correlation between G α (340–350) and R*-loops, and ones with unfavorable charge interactions were discarded. At every translation, the 10 best-scoring

complexes were kept for further evaluation. There were usually more than 3000 structures at this step. To extract feasible structures, the following filtering procedure was employed. First, complexes where Cys347, Leu349, or Phe350 of G α (340–350) were in contact with any atom(s) in R*-loops were retained in accord with experimental observation, which assures that G α would be in the right orientation; i.e., the rest of G α is placed in the cytoplasm. Second, two potential binding sites on R*, formed by loops 2 and 3 and by loops 3 and 4, were explored based on mutational studies (Acharya et al., 1997; Marin et al., 2000; Ernst et al., 2000). Complexes where Val138 or Val139 of R* was in contact with any atom(s) in G α (340–350) for the first binding mode, and anywhere in the R*-segments of Asn310-Gln312 and Lys245-Gln247 were in proximity to G α (340–350) for the second binding mode, were kept for further evaluations. Finally, the crystal structures of G $\alpha\beta\gamma$ -trimer (Lambright et al., 1996) and the modeled R* were fused with G α (340–350) and the R*-loops in the complexes, and any structures with G α -R* collisions were discarded as physically impossible. For comparisons, the same procedure was performed with G α (340–350) and the loop-complex derived from dark-adapted rhodopsin.

Binding-affinity prediction

The binding affinities of the analog peptides as well as G α (340–350) were calculated. The structures of the peptides were aligned with G α (340–350) in the docked complexes, and the structures of the interfaces between R* and the peptides were energy minimized using Macromodel 6.5 (Mohamadi et al., 1990) with the Amber94 force field (Cornell et al., 1995). The VALIDATE program (Head et al., 1996) was then used to calculate the properties of the minimized complexes, charges, induction energy, and hydrophobic/hydrophilic contact-surface that were used to estimate the binding affinities. The partial least square of latent variables (PLS) (Wold et al., 1993) model of affinity calibrated with 65 crystalline complexes of known affinities available in VALIDATE was applied to the modeled complexes, and the binding affinities of the peptides were predicted. All the calculations were carried out on Silicon Graphics Indigo R4000 and R10000 workstations.

RESULTS

Fig. 1 shows the measurements and the fitted dose-response curves for active peptides. The EC₅₀ values for all the analog peptides were calculated and listed in Table 1. No Meta II stabilization effect was observed for the analogs marked as $\gg 10$ mM, up to 5 mM concentration. Fig. 2 shows the structural changes in the crystal structure of rhodopsin proposed to occur upon activation to generate the R* state based on imposing the changes in distances seen by the EPR measurements. Seven complex structures were found by molecular docking of G α (340–350) into the modeled R*-loops as shown in Fig. 3, whereas docking with R-loops derived from the crystal structure yielded none. The measured binding affinities were compared with the predictions to evaluate the structures derived by molecular modeling. Fig. 4 shows the comparisons for the seven complexes (*a–g*) and a control complex (*h*), where the N-terminus of the peptide that connects to the rest of G α is pointing into the binding pocket. The values of the experimental data for inactive analogs ($\gg 10$ mM) were set to zero; i.e., EC₅₀ = 1 M. To quantitatively compare the modeled structures, correlation coefficients were calculated between predicted and observed affinities. Listed in Table 3 are the correlation coefficients for

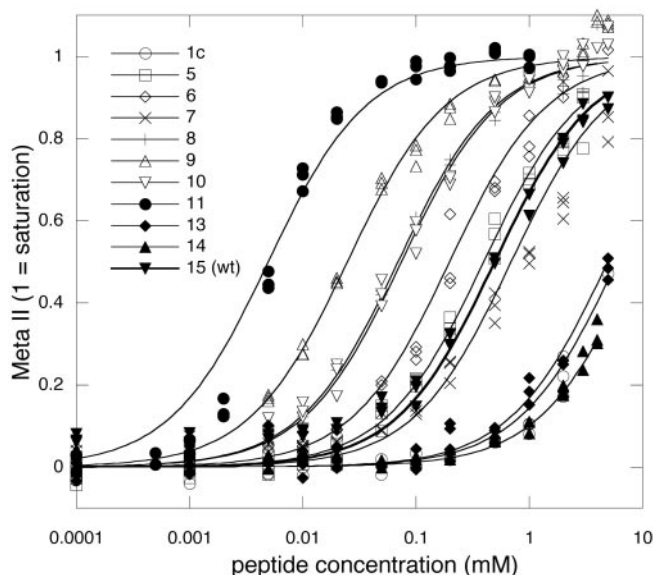


FIGURE 1 Dose-responses of Meta II stabilization for the active analogs (1c, 5, 6, 7, 8, 9, 10, 11, 13, and 14) and $G_{\alpha}(340-350)$ normalized by the saturation level. Measurements were fitted with the equation: $\text{Meta II} = \text{peptide concentration}/(\text{peptide concentration} + EC_{50})$ to obtain EC_{50} values of the peptides.

all the analogs, and with the inactive analogs (no experimental measurement of affinity) excluded.

DISCUSSION

Constrained analogs of the $G_{\alpha}(340-350)$

As seen with analogs 6, 9, 10, and 11, enhancing the hydrophobicity of the hydrophobic cluster at the C-cap turn

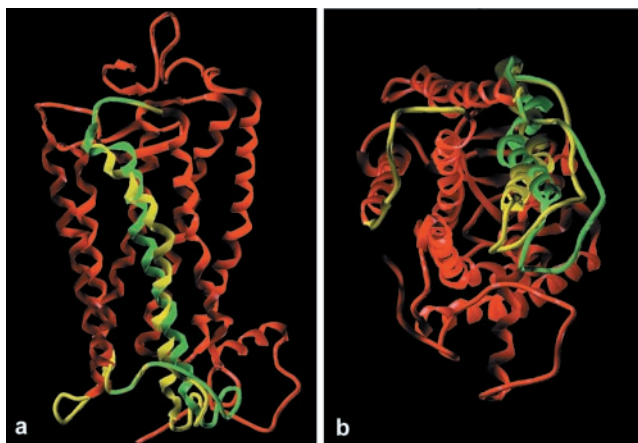


FIGURE 2 Probable structural change of rhodopsin induced by light activation. Helix 6 was moved (R:yellow > R*:green) as suggested by the distance measurement by EPR (Farrens et al., 1996). (a) Side view; (b) View from cytoplasmic space. The opening between cytoplasmic loops 2 (shown in yellow) and 3 (yellow > green) widens with this structural change, creating a probable binding site for the α -subunit of transducin.

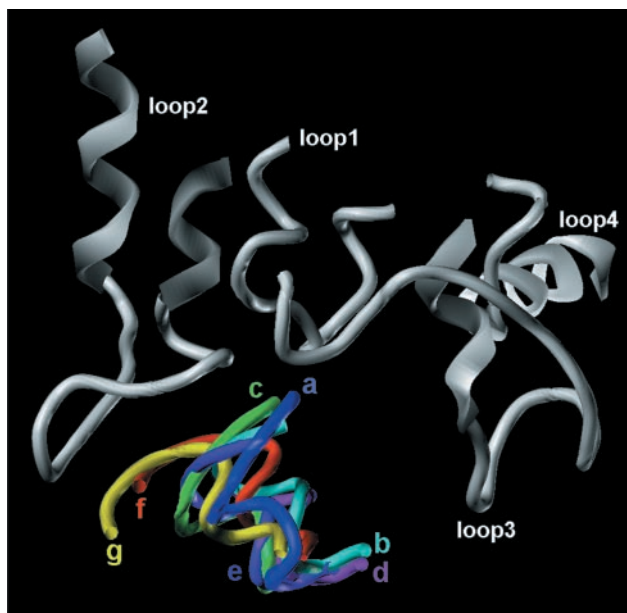


FIGURE 3 Structures of the complex between $G_{\alpha}(340-350)$ and cytoplasmic loops of R* consisting of Tyr60-Leu76, Val130-Thr160, Gln225-Arg252, and Ile305-Cys322, obtained by molecular docking (Gabb et al., 1997). The surface correlation between R*-loops and $G_{\alpha}(340-350)$ was scored for each of seven model complexes by FTDOCK as follows (in arbitrary units): 53 (a), 51 (b), 46 (c), 45 (d), 37 (e), 36 (f), and 29 (g).

by changing residues into more hydrophobic amino acids improved activities, suggesting that hydrophobic interaction of this moiety of $G_{\alpha}(340-350)$ with R* is the driving force for R* binding. The higher activity of analog 9 over 10 may indicate that a specific interaction between the carboxyl group of Phe350 and R* exists, consistent with a previous study (Osawa and Weiss, 1995). Analog 7 with rather strong helical constraints retained almost full activity, confirming the TrNOE structure (Kisselev et al., 1998) and the insignificance of the side chains of Ile340, Glu342, and Asn343 in specific interactions. The improved affinity of analog 8 where the helical turn of Glu342-Lys345 was locked by the amide bond indicates that preorganization of the receptor-bound conformation is beneficial. Analog 12 with a point mutation of Cys347Ser completely lost its activity. Also, all the analog peptides with the sulfhydryl of Cys347 blocked due to the intrapeptide disulfide bonds (analogs 1c, 2c, and 6c) showed very little activity, if any. Furthermore, the activity of $G_{\alpha}(340-350)$ was lower ($EC_{50} \approx 1$ mM, data not shown) when the assay was done without DTT. This can be explained as a result of oxidation of the sulfhydryl at Cys347 to form disulfide dimers, as pH 8 favors sulfhydryl oxidation. These results strongly argue that Cys347 is an important recognition site for R* binding. Analog 3 was inactive presumably due to its Cys347Pro substitution, not to the helical constraint or the extra volume requirements of D-NMeAla. The 3Mpt347 in analog 4 has a sulfhydryl group, but the five-membered ring of proline to which the

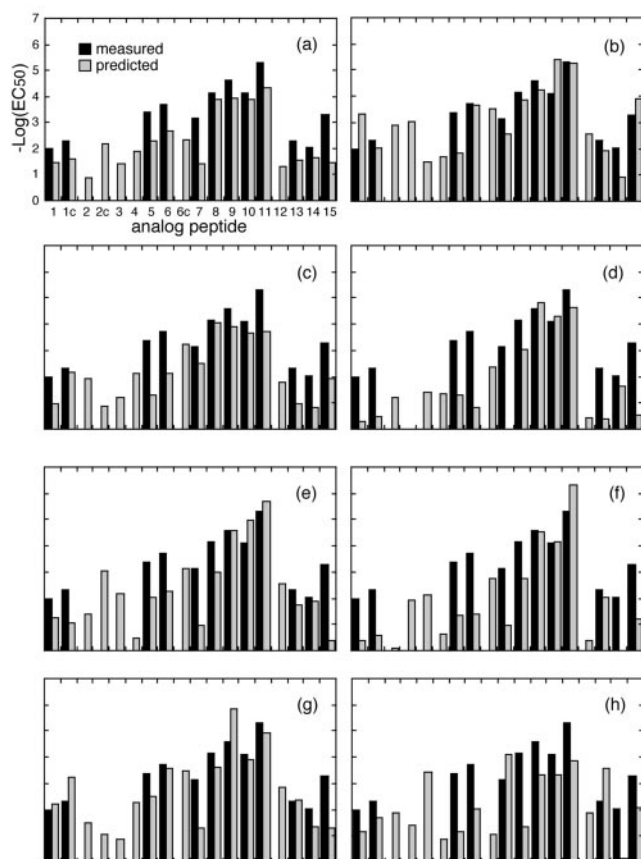


FIGURE 4 Comparisons between measured (*solid bars*) and predicted (*hatched bars*) affinities of the peptides for models (*a–h*). Measurements for the inactive analogs (2, 2c, 3, 4, 6c, and 12) were set to $EC_{50} = 1$ M. VALIDATE (Head et al., 1996) was used to predict affinities.

sulfhydryl is attached is highly constrained. Therefore, it is likely that the sulfhydryl is not pointing in the right direction to correctly interact with R^* or that the increased steric bulk of the analog is not tolerated by R^* . In this study, our attempt to constrain the C-cap turn (analogs 1c and 2c) failed because of the loss of Cys347 side chains due to the intrapeptide disulfide bonds. However, we have recently shown that a cyclic peptide with amide bond between Phe350 (NH_2 at the *para* position of the phenyl ring) and

TABLE 3 Correlation coefficients between the prediction and the experiment

Model	All analogs	Active analogs
a	0.71	0.90
b	0.57	0.79
c	0.54	0.86
d	0.56	0.81
e	0.45	0.80
f	0.58	0.89
g	0.61	0.75
Control	0.41	0.50

the Glu341 carboxyl group stabilizing the reverse turn had significantly improved binding affinity (Sha et al., 2001). Leu349 was found to be another invariable residue as previously reported (Osawa and Weiss, 1995). Mutations of Leu349Pen in analog 1, Leu349Cys in analog 2, Leu349Ile in analog 13, and Leu349Tle in analog 14 all significantly reduced activities. This result is particularly striking because leucine, isoleucine, and *tert*-leucine are isomers, so that their chemical properties are quite similar. They differ only in their arrangement of the carbon backbone in the side chains, leading to the hypothesis that the side chain of Leu349 is in intimate contact with R^* .

In summary, from the point of $G_t\alpha(340–350)$, hydrophobic interaction between the binding site on R^* and the hydrophobic cluster at the C-cap turn is the major force for the binding, and Cys347 and Leu349 seem to have direct surface contact with photoactivated rhodopsin.

Model of photoactivated rhodopsin

In adapting the crystal structure of dark-adapted rhodopsin to the photoactivated state (R^*), helix 6 was rotated and tilted outward centered near Ile275- $C\alpha$ at the extracellular end of helix 6. As a result of this movement, the opening between the cytoplasmic loops 2 and 3 was widened, which we believe creates the binding site for G_t . Although the cytoplasmic end of helix 6 changed its location by ~ 5 Å, the translational movement of the extracellular end was only ~ 0.4 Å. The rest of the molecule was kept unchanged. We have chosen to move only helix 6 because this is the only part of the R^* for which movement is supported by quantitative experimental data. Struthers et al. (2000) showed that a highly constrained rhodopsin, in which four disulfide bonds were restricting the movements of the helices, could activate G_t , indicating that in the cytoplasmic side, only helices 2, 4, and/or 6 were required to move for active R^* formation. Yang et al. (1996) observed that the cytoplasmic ends of helices 1 and 6 moved apart by 5 Å upon light activation, but the experiment by Struthers et al. (2000) showed that this movement is not a requirement. It is quite possible that other helices also move, and there exists some circumstantial evidence (Abdulaev and Ridge, 1998; Borhan et al., 2000; Farahbakhsh et al., 1995), but the movement cannot be determined quantitatively for molecular modeling at this time. In accord with the model, the EPR experiments of Delmelle and Virmaux (1977) showed no changes in the distance between a spin label on Cys140 at the C-terminus of helix 3 and another spin label on Cys316 in the middle of helix 8 upon light activation. One must remember, however, that the absence of detection of movement may simply reflect the lack of sufficient sensitivity using the spin-label approach. Another reason that a movement of helix 6 is plausible is that helix 6 contains Trp265, which forms a cross-link with a photoaffinity analog of the ionone ring of 11-*cis* retinal in R . When light energy isomerizes 11-*cis* retinal to all-*trans* retinal, the cross-link to helix 6 is not formed, and the ionone ring

points instead toward helix 4 (Borhan et al., 2000). The distances between Val139 and Lys248-Arg252 in the modeled R* structure are listed in the column 5 of Table 2. The root mean square error from the estimated target distances was 1.1 Å.

Model of R*/Gt α (340–350) complex

Apparently, the movement of helix 6 according to experimental data generated a reasonable model of light-activated rhodopsin as it successfully created a binding site for G α (340–350) in accord with experimental observation (Franke et al., 1990; Acharya et al., 1997). In all of the resultant complexes, G α (340–350) binds to the site in between loops 2 and 3, indicating there is not enough space between loops 3 and 4 in our R*-model for complex formation. The seven binding modes differ basically in the orientation around the helical axis of G α (340–350) and can be sorted into three structural groups. In complexes b, d, and e, the C-terminus is pointing toward the bottom of helix 6, Glu247-Lys248. Leu349 and Phe350 are well in the pocket formed by loops 2 and 3, and closer to loop 2 rather than loop 3. In the second structural group, consisting of a and c, G α (340–350) is turned slightly clockwise (viewed from the cytoplasmic side), compared with the first group, into the binding pocket, bringing Leu349 close to the N-end of loop 3. In complexes f and g, G α (340–350) is further turned clockwise until its C-terminus points away from the binding pocket. Cys347-Leu349 is close to the amino end of loop 2, but loop 3 is now distant from any part of the peptide. There is a cluster of hydrophobic residues in the binding site (137VVVC140) appropriate for the hydrophobic interaction with G α , consistent with the experimental results. Leu349, as being close to the helical axis, is in the binding pocket in all models, and Cys347 is within the binding site in two of the models, g and f.

Koenig et al. (2000) reported that the N-H vectors of Leu344 and Gly348 make angles of $48 \pm 4^\circ$ and $40 \pm 8^\circ$, respectively, with the disk normal by measuring residual dipolar coupling between rhodopsin-containing disk membrane and an analog peptide (IRENLKDSGLF). Complexes a, f, and g are in relatively good agreement (L344: 60° , 52° , 52° ; G348: 49° , 36° , 42° , respectively), and in the other complexes, the angles are more than 20° off for Leu344 and 10° off for Gly348. Because it is unclear how the mutations of Lys341Arg and Cys347Ser affected the R* binding and/or the bound structure of the peptide, and the membrane's relative location to rhodopsin contained error in our angle measurement (helix 4 was used as the membrane normal), this experimental result does not necessarily disprove models that do not quantitatively agree.

There have been mutational studies (Acharya et al., 1997) identifying Tyr136-Val139 in loop 2 and Glu247-Thr251 in loop 3 as interaction sites with G α . Khorana's group showed that Glu342-Lys345 (as well as Leu19-Arg28 and Arg310-Lys313) of G α cross-linked to Ser240Cys in loop 3 of rhodopsin upon light activation

(Cai et al., 2001; Itoh et al., 2001). All of the modeled complexes possibly have interactions between G α (340–350) and loop 2 and/or loop 3 because of the way the docked structures were filtered (see Experimental Procedures); particularly Tyr137-Val139 seems to be literally facing the hydrophobic cluster of G α (340–350). Another study (Ernst et al., 2000; Marin et al., 2000) has shown that Asn310-Gln312, the amino end of helix 8, interacts with G α (340–350). Obviously, in none of the complexes would G α (340–350) be able to directly interact with helix 8. As it is difficult to distinguish between direct and indirect effects from mutational studies, our models do not necessarily conflict with these experimental results. It is quite possible that the interaction of G α with loop 3 causes conformational changes in helix 8. Or else, helix 8 is holding loop 3 stabilizing the binding pocket as the structural change proposed here brings loop 3 closer to the N-terminus of helix 8; therefore, rhodopsin with mutation in helix 8 may fail to form the binding site.

The C-terminal region of G $\alpha\gamma$ is also known to bind to photoactivated rhodopsin and stabilize Meta II conformation (Kisselev et al., 1995). However, in our models, the γ -subunit would not be able to contact with the receptor, regardless of the peptide orientation. The distance between C-termini of the α -subunit and γ -subunit is ~ 45 Å as measured in the crystal structure of G $\alpha\beta\gamma$ heterotrimer (Lambright et al., 1996), whereas the receptor is 43 Å across (radius < 22 Å). One possible explanation for this discrepancy is sequential binding of the two sites (Kisselev et al., 1999). Receptor dimerization is another possibility; there may be an adjacent rhodopsin for direct interaction with the γ -subunit, next to the one bound to the α -subunit.

Evaluation of the models

Although the accuracy of absolute affinity prediction is problematic, prediction of relative affinities is more reliable. Thus, the overall correlation between predicted affinity and experimental observation of a series of active analogs could be used to estimate the probability that a given binding mode is plausible. The strongest correlation to the experimental data seen in Table 3 was found with complex a, using either way of treating the data (either including the inactive analogs or not). It is also the complex of best surface correlation, supporting the hypothesis that the hydrophobic interaction is crucial. The control complex with the peptide orienting the α -subunit to overlap the receptor shows the weakest correlation as expected, and its value (~ 0.5) can roughly estimate the noise level of this procedure, below which a critical evaluation cannot be made. When the inactive analogs were excluded, discrimination of control complex against the plausible structures became much more obvious, and two additional complexes (c and f) show strong correlation to the experimental data as well as does complex a. Presumably, the values with only the active

analogs are more reliable than values with all analogs because 1) the binding affinities for the inactive analogs (zero) are not measured values, but lack of activity at an arbitrary concentration limitation and 2) lack of measured activity of some analogs may be due to experimental conditions (limited solubility, for example). After all, in the case that a ligand does not bind to the receptor, which we observed for the analogs missing the Cys347 side chain, the affinity prediction based on the structure of the complex is not useful. The role of Cys347 side chain might be a necessary recognition site in an earlier stage of the binding process, rather than stabilizing the final complex; thus the locations of Cys347 in all models do not correlate with the experimental observation suggesting that the sulfhydryl group of Cys347 is in intimate contact with R*.

The correlation coefficients of a, c, and f are quite close, indicating that the sensitivity of this model-evaluation process is not sufficient to determine the precise orientation of G_iα(340–350) in the binding pocket. This problem may be overcome by testing additional analogs, thus widening the variety in the surface structures of analogs probing the receptor cavity, because the relative orientations of the peptides within the cavity make differences in the properties of the complex that VALIDATE computes (Head et al., 1996). Determining the precise orientation of G_iα would greatly help us to understand the relative orientation of the rhodopsin with respect to transducin in the complex and impose constraints on possible receptor-dimer formation. Yet, the binding site on R* seems to be confirmed by the experimental results, as the modeled complexes show such a strong correlation to the measurement for as many as 18 (12 active) analog peptides of wide affinity (5 μM to 10 mM, 2000-fold range in activities).

CONCLUSIONS

A comprehensive approach utilizing biophysical measurements (both crystal and TrNOE structures and EPR-distance measurements), structure-activity studies, molecular modeling, and affinity prediction yields plausible structural models of the interaction between R* and transducin. The exposure of a binding site and strong correlation between experimental and estimated affinity found for the set of constrained peptide analogs supports the low-resolution model of the photoactivated state generated from the crystal structure of dark-adapted rhodopsin by movement of helix 6. The resultant hypothetical complexes are consistent with a number of experimental data from mutational studies on both transducin and rhodopsin as well as biophysical studies measuring the orientation of NH vectors of the bound G_iα-peptide (Koenig et al., 2000) not used in their construction. These models provide guides in designing experiments to further explore the details of the mechanism of signal transduction that should eventually enable us to control these clinically important systems. For example, distance measurements between certain atoms will be able to orient G_i correctly in the binding pocket. The distance between

specific sites can be estimated by NMR, EPR, and various cross-linking techniques using derivatized rhodopsin, transducin, and synthetic peptides (work in progress). Finally, this comprehensive approach to evaluating protein complexes can be applied to other systems where direct structural-determination methods (x-ray crystallography and NMR spectroscopy) are problematic.

We acknowledge support for this research from National Institutes of Health grant EY12113. R.A. is a graduate student in the Biomedical Engineering Program at Washington University. The Washington University Mass Spectroscopy Resource Center supported by National Institutes of Health (RR00954) was used to characterize the constrained analogs synthesized as part of this study.

REFERENCES

- Abdulaev, N. G., and K. D. Ridge. 1998. Light-induced exposure of the cytoplasmic end of transmembrane helix seven in rhodopsin. *Proc. Natl. Acad. Sci. U.S.A.* 95:12854–12859.
- Acharya, S., Y. Saad, and S. S. Karnik. 1997. Transducin-alpha C-terminal peptide binding site consists of C-D and E-F loops of rhodopsin. *J. Biol. Chem.* 272:6519–6524.
- Aris, L., A. Gilchrist, S. Rens-Domiano, C. Meyer, P. J. Schatz, E. A. Dratz, and H. E. Hamm. 2001. Structural requirements for the stabilization of metarhodopsin II by the carboxyl terminus of the alpha subunit of transducin. *J. Biol. Chem.* 276:2333–2339.
- Borhan, B., M. L. Souto, H. Imai, Y. Shichida, and K. Nakanishi. 2000. Movement of retinal along the visual transduction path. *Science*. 288:2209–2212.
- Cai, K., Y. Itoh, and F. C. Khorana. 2001. Mapping of contact sites in complex formation between transducin and light-activated rhodopsin by covalent crosslinking: use of a photoactivatable reagent. *Proc. Natl. Acad. Sci. U.S.A.* 98:4877–4882.
- Chalmers, D. K., and G. R. Marshall. 1995. Pro-D-NMe-amino acid and D-pro-NMe-amino acid: simple, efficient reverse-turn constraints. *J. Am. Chem. Soc.* 117:5927–5937.
- Coleman, D. E., and S. R. Sprang. 1998. Crystal structures of the G protein Gi alpha 1 complexed with GDP and Mg²⁺: a crystallographic titration experiment. *Biochemistry*. 37:14376–14385.
- Cornell, W. D., P. Cieplak, C. I. Bayly, I. R. Gould, K. M. Merz, D. M. Ferguson, D. C. Spellmeyer, T. Fox, J. W. Caldwell, and P. A. Kollman. 1995. A 2nd generation force-field for the simulation of proteins, nucleic-acids, and organic-molecules. *J. Am. Chem. Soc.* 117:5179–5197.
- Delmelle, M., and N. Virmaux. 1977. Location of two sulfhydryl groups in the rhodopsin molecule by use of the spin label technique. *Biochim. Biophys. Acta.* 464:370–377.
- Dratz, E. A., J. E. Furstenau, C. G. Lambert, D. L. Thireault, H. Rarick, T. Schepers, S. Pakhlevanians, and H. E. Hamm. 1993. NMR structure of a receptor-bound G-protein peptide. *Nature*. 363:276–281.
- Dratz, E. A., L. E. Furstenau, C. G. Lambert, D. L. Thireault, H. Rarick, T. Schepers, S. Pakhlevanians, and H. E. Hamm. 1997. NMR structure of a receptor-bound G-protein peptide. *Nature*. 390:424.
- Ernst, O. P., C. K. Meyer, E. P. Marin, P. Henklein, W. Y. Fu, T. P. Sakmar, and K. P. Hofmann. 2000. Mutation of the fourth cytoplasmic loop of rhodopsin affects binding of transducin and peptides derived from the carboxyl-terminal sequences of transducin alpha and gamma subunits. *J. Biol. Chem.* 275:1937–1943.
- Farahbakhsh, Z. T., K. D. Ridge, H. G. Khorana, and W. L. Hubbell. 1995. Mapping light-dependent structural changes in the cytoplasmic loop connecting helices C and D in rhodopsin: a site-directed spin labeling study. *Biochemistry*. 34:8812–8819.

- Farrens, D. L., C. Altenbach, K. Yang, W. L. Hubbell, and H. G. Khorana. 1996. Requirement of rigid-body motion of transmembrane helices for light activation of rhodopsin. *Science*. 274:768–770.
- Franke, R. R., B. Konig, T. P. Sakmar, H. G. Khorana, and K. P. Hofmann. 1990. Rhodopsin mutants that bind but fail to activate transducin. *Science*. 250:123–125.
- Gabb, H. A., R. M. Jackson, and M. J. Sternberg. 1997. Modelling protein docking using shape complementarity, electrostatics and biochemical information. *J. Mol. Biol.* 272:106–120.
- Galaktionov, S., G. V. Nikiforovich, and G. R. Marshall. 2001. Ab initio modeling of small, medium and large loops in proteins. *Biopolymers*. 60:153–168.
- Goodsell, D. S., and A. J. Olson. 1990. Automated docking of substrates to proteins by simulated annealing. *Proteins*. 8:195–202.
- Guarnieri, F., and W. C. Still. 1994. A rapidly convergent simulation method: mixed Monte Carlo/stochastic dynamics. *J. Comput. Chem.* 15:1302–1310.
- Hall, D., and N. Pavitt. 1984. An appraisal of molecular force fields for the representation of polypeptides. *J. Comput. Chem.* 5:441.
- Hamm, H. E., D. Deretic, A. Arendt, P. A. Hargrave, B. Koenig, and K. P. Hofmann. 1988. Site of G protein binding to rhodopsin mapped with synthetic peptides from the alpha subunit. *Science*. 241:832–835.
- Hargrave, P. A., H. E. Hamm, and K. P. Hofmann. 1993. Interaction of rhodopsin with the G-protein, transducin. *Bioessays*. 15:43–50.
- Head, R. D., M. L. Smythe, T. I. Oprea, C. L. Waller, S. M. Green, and G. R. Marshall. 1996. VALIDATE: a new method for the receptor-based prediction of binding affinities of novel ligands. *J. Am. Chem. Soc.* 118:3959–3969.
- Hodgkin, E. E., J. D. Clark, K. R. Miller, and G. R. Marshall. 1990. Conformational analysis and helical preferences of normal and α , α -dialkyl amino acids. *Biopolymers*. 30:533–546.
- Itoh, Y., K. Cai, and H. G. Khorana. 2001. Mapping of contact sites in complex formation between light-activated rhodopsin and transducin by covalent crosslinking: use of a chemically preactivated reagent. *Proc. Natl. Acad. Sci. U.S.A.* 98:4883–4887.
- Kisselev, O., M. Ermolaeva, and N. Gautam. 1995. Efficient interaction with a receptor requires a specific type of prenyl group on the G protein gamma subunit. *J. Biol. Chem.* 270:25356–25358.
- Kisselev, O. G., J. Kao, J. W. Ponder, Y. C. Fann, N. Gautam, and G. R. Marshall. 1998. Light-activated rhodopsin induces structural binding motif in G protein alpha subunit. *Proc. Natl. Acad. Sci. U.S.A.* 95:4270–4275.
- Kisselev, O. G., C. K. Meyer, M. Heck, O. P. Ernst, and K. P. Hofmann. 1999. Signal transfer from rhodopsin to the G-protein: evidence for a two-site sequential fit mechanism. *Proc. Natl. Acad. Sci. U.S.A.* 96:4898–4903.
- Koenig, B. W., D. C. Mitchell, S. Konig, S. Grzesiek, B. J. Litman, and A. Bax. 2000. Measurement of dipolar couplings in a transducin peptide fragment weakly bound to oriented photo-activated rhodopsin. *J. Biomol. NMR*. 16:121–125.
- Kolodziej, S. A., G. V. Nikiforovich, R. Skeean, M.-F. Lignon, J. Martinez, and G. R. Marshall. 1995. Ac-[3- and 4-alkylthiopropyl]-CCK₄ analogs: synthesis and implications for the CCK-B receptor-bound conformation. *J. Med. Chem.* 38:137–149.
- Lambright, D. G., J. Sondek, A. Bohm, N. P. Skiba, H. E. Hamm, and P. B. Sigler. 1996. The 2.0 Å crystal structure of a heterotrimeric G protein. *Nature*. 379:311–319.
- Marin, E. P., K. G. Krishna, T. A. Zvyaga, J. Isele, F. Siebert, and T. P. Sakmar. 2000. The amino terminus of the fourth cytoplasmic loop of rhodopsin modulates rhodopsin-transducin interaction. *J. Biol. Chem.* 275:1930–1936.
- Marshall, G. R., and H. E. Bosshard. 1972. Angiotensin II: studies on the biologically active conformation. *Circ. Res.* 31(Suppl. 2):143–150.
- Martin, E. L., S. Rens-Domiano, P. J. Schatz, and H. E. Hamm. 1996. Potent peptide analogues of a G protein receptor-binding region obtained with a combinatorial library. *J. Biol. Chem.* 271:361–366.
- Meng, E. C., B. K. Shoichet, and I. D. Kuntz. 1992. Automated docking with grid-based energy evaluation. *J. Comput. Chem.* 13:505–524.
- Miranda, A., S. L. Lahrichi, J. Gulyas, S. C. Koerber, A. G. Craig, A. Corrigan, C. Rivier, W. Vale, and J. Rivier. 1997. Constrained corticotropin-releasing factor antagonists with $i-(i + 3)$ Glu-Lys bridges. *J. Med. Chem.* 40:3651–3658.
- Mohamadi, F., N. G. J. Richards, W. C. Guida, R. Liskamp, M. Lipton, C. Caufield, G. Chang, T. Hendrickson, and W. C. Still. 1990. MacroModel: an integrated software system for modeling organic and bioorganic molecules using molecular mechanics. *J. Comput. Chem.* 11:440–467.
- Moult, J., T. Hubbard, K. Fidelis, and J. T. Pedersen. 1999. Critical assessment of methods of protein structure prediction (CASP): round III. *Proteins*. Suppl 3:2–6.
- Osawa, S., and E. R. Weiss. 1995. The effect of carboxyl-terminal mutagenesis of Gt alpha on rhodopsin and guanine nucleotide binding. *J. Biol. Chem.* 270:31052–31058.
- Palczewski, K., T. Kumasaka, T. Hori, C. A. Behnke, H. Motoshima, B. A. Fox, I. Le Trong, D. C. Teller, T. Okada, R. E. Stenkamp, M. Yamamoto, and M. Miyano. 2000. Crystal structure of rhodopsin: a G protein-coupled receptor. *Science*. 289:739–745.
- Papernmaster, D. S., and W. J. Dreyer. 1974. Rhodopsin content in the outer segment membranes of bovine and frog retinal rods. *Biochemistry*. 13:2438–2444.
- Phillips, W. J., and R. A. Cerione. 1994. A C-terminal peptide of bovine rhodopsin binds to the transducin alpha-subunit and facilitates its activation. *Biochem. J.* 299:351–357.
- Schellman, C. 1980. The α_L conformation at the ends of helices. In Protein Folding. R. Jaenicke, editor. Elsevier/North-Holland Biomedical Press, Amsterdam. 53–61.
- Sha, W., R. Arimoto, and G. R. Marshall. 2001. Receptor-bound conformation of α -peptide of transducin (Gt) is not stabilized by a π -cation interaction but by constrained lactam bridges between residues 341 and 350. In Proc. 2nd Int./17th Am. Peptide Symp. R. A. Houghton and M. Lebl, editors. American Peptide Society, San Diego, CA. In press.
- Still, W. C., A. Tempczyk, R. C. Hawley, and T. Hendrickson. 1990. Semianalytical treatment of solvation for molecular mechanics and dynamics. *J. Am. Chem. Soc.* 112:6127–6129.
- Struthers, M., H. Yu, and D. D. Oprian. 2000. G protein-coupled receptor activation: analysis of a highly constrained, “straitjacketed” rhodopsin. *Biochemistry*. 39:7938–7942.
- Takemoto, D. J., D. Morrison, L. C. Davis, and L. J. Takemoto. 1986. C-terminal peptides of rhodopsin: determination of the optimum sequence for recognition of retinal transducin. *Biochem. J.* 235:309–312.
- Takeuchi, Y., and G. R. Marshall. 1998. Conformational analysis of reverse-turn constraints by N-methylation and N-hydroxylation of amide bonds in peptides and non-peptide mimetics. *J. Am. Chem. Soc.* 120:5363–5372.
- Tesmer, J. J., D. M. Berman, A. G. Gilman, and S. R. Sprang. 1997. Structure of RGS4 bound to AIF4-activated G(i alpha1): stabilization of the transition state for GTP hydrolysis. *Cell*. 89:251–261.
- Vakser, I. A. 1996. Low-resolution docking: prediction of complexes for undetermined structures. *Biopolymers*. 39:455–464.
- Wall, M. A., D. E. Coleman, E. Lee, J. A. Iniguez-Lluhi, B. A. Posner, A. G. Gilman, and S. R. Sprang. 1995. The structure of the G protein heterotrimer Gi alpha 1 beta 1 gamma 2. *Cell*. 83:1047–1058.
- Wold, S., E. Johansson, and M. Cocchi. 1993. PLS-partial least-squares projections to latent variables. In 3D QSAR in Drug Design. H. Kubinyi, editor. ESCOM Science Publishers, Leiden, The Netherlands. 523–550.
- Yamazaki, A., F. Bartucca, A. Ting, and M. W. Bitensky. 1982. Reciprocal effects of an inhibitory factor on catalytic activity and noncatalytic cGMP binding sites of rod phosphodiesterase. *Proc. Natl. Acad. Sci. U.S.A.* 79:3702–3706.
- Yang, K., D. L. Farrens, C. Altenbach, Z. T. Farahbakhsh, W. L. Hubbell, and H. G. Khorana. 1996. Structure and function in rhodopsin: cysteines 65 and 316 are in proximity in a rhodopsin mutant as indicated by disulfide formation and interactions between attached spin labels. *Biochemistry*. 35:14040–14046.